JOURNAL OF AIRCRAFT
Vol. 31, No. 1, Jan.–Feb. 1994

Panel Flutter Suppression Using Adaptive Material Actuators

R. C. Scott*
NASA Langley Research Center, Hampton, Virginia 23681
and
T. A. Weisshaar†
Purdue University, West Lafayette, Indiana 47907

Piezoelectrics and shape memory alloys may be used as integrated actuators to control supersonic flutter of flat panels because panel strain and stiffness can be actively controlled. This article uses a Rayleigh-Ritz panel flutter model to analyze the effectiveness of integrated segmented actuators to control panel bending deformation and in-plane forces, and increase the flutter speed of the panels. A nondimensional parameter for actuator effectiveness is presented to help evaluate the effectiveness of different materials and their placement in the panel. These studies suggest that creating and controlling in-plane panel forces will provide the most effective control of panel flutter. In addition, tradeoffs between actuator stiffness and electromechanical properties are illustrated.

Nomenclature

a = panel streamwise dimension
$[B_{ij}]$ = aerodynamic stiffness matrix
b = panel width
D_{ij} = plate bending stiffness element
d_{ij} = piezoelectric strain/charge constants
E_p = Young's modulus of adaptive material
E_s = Young's modulus of substructure material
E_3 = electric field, voltage per unit length, V/T_p
E_3^* = maximum electric field before depoling
$[K_{ij}]$ = panel stiffness matrix
M = freestream Mach number
m_0 = panel mass per unit area
NC = number of panel actuators
P = nondimensional piezoelectric effectiveness parameter
q = dynamic pressure, $\frac{1}{2}\rho U^2$
T = panel total thickness
T_p = thickness of actuator layer
U = freestream velocity
U_{cr} = flutter velocity
U_{sat} = control saturation velocity
u_s = nondimensional control parameter
V = voltage across acuator surfaces
w = panel displacement out-of-plane
Λ = actuation strain
λ = dynamic pressure parameter, $2q/D(M^2 - 1)^{1/2}$
λ_{cr} = value of λ at flutter
λ_{sat} = control saturation value of λ
ρ = freestream air density

Introduction

HIGH-SPEED cruise aircraft and re-entry vehicles operate in an extreme environment that places severe thermal and structural demands on thin, external aerostructural surfaces. Surface skin panels are designed for strength, buckling, and fatigue resistance, and checked for panel flutter. Panel flutter is a self-excited, dynamic instability of thin plate or shell-like components of flight vehicles in the supersonic flight regime. Prevention of panel flutter may require additional weight to increase the panel stiffness. If panel flutter is discovered during a flight test, a micro-actuator, such as that discussed in this article, might quickly cure the problem without extensive redesign.

The objective of this article is to examine the use of piezoelectric materials and shape memory alloys to control the flutter dynamic pressure of a flat, simply supported rectangular panel with one panel surface immersed in a supersonic flow. Two specific questions will be addressed. The first is how to integrate the actuator materials into the structure effectively, i.e., where to place them and how to segment them over the surface. The answer to this question requires the study of tradeoffs between the effectiveness of adding a complex actuator to the panel or simply increasing its thickness. The second question to be addressed is how to control the panel response, i.e., whether to control panel stiffness by changing the panel bending stiffness or whether to control response by controlling in-plane stiffness.

Background

Modern aerospace vehicles have a multitude of different design requirements, some of which conflict with each other. As a result, to satisfy requirements in one area, performance in another often must be sacrificed. Ultimately, the various design objectives are prioritized for the given aircraft mission. The final multifunctional design will reflect these priorities and the tradeoffs between wide-ranging design objectives. As a result, the vehicle design may not be optimal in any one area.

Advanced composite materials have helped designers to reduce the penalties introduced by multifunctional requirements. These materials provide additional design freedoms to tailor load paths and stiffness, and allow balancing of opposing design goals by optimizing or "tailoring" the structural layout.[1] On the other hand, no matter how effective design optimization strategies may be, they have limits. Structural optimization also provides a structural design that is time invariant and cannot respond or adapt to changing flight conditions.

Adaptive designs—designs whose configuration changes during flight—can resolve some conflicting design require-

Presented as Paper 91-1067 at the AIAA/ASME/ASCE/AHS/ASC 32nd Structures, Structural Dynamics, and Materials, Baltimore, MD, April 8–10, 1991; received June 13, 1991; revision received Oct. 22, 1992; accepted for publication Nov. 3, 1992.

*Aerospace Engineer, M/S 340. Member AIAA.
†Professor, School of Aeronautics and Astronautics. Fellow AIAA.

ments. For instance, military aircraft may use variable sweep wings to be efficient in both subsonic and supersonic flight. At low speeds, most aircraft use flaps to change wing camber at flight conditions requiring different geometry, such as landing and cruise. To be adaptive, wings use mechanical actuators, hydraulic fluid, and movable parts to change their configuration.

A relatively new concept in structural design incorporates so-called "adaptive" or "smart" materials into the structure.[2] These active structural elements sense structural response and then respond to the multifunctional requirements of the design. The result has been called a smart structure, an intelligent structure, or an adaptive structure. Whatever the name, the result is an active structure with integrated sensors, actuators, and special processors that allow the structure to take on functions beyond the traditional mission of carrying a load or providing a volumetric shape. We will use the terms adaptive material and adaptive structure in this article to identify materials and structural forms that actively control the structural response.

Adaptive material actuators include piezoelectrics, shape memory alloys, magnetostrictors, electrostrictors, and electrorheological fluids. Piezoelectric materials are used as sensors and actuators in active structures and use electrical field as a stimulus. On the other hand, shape memory alloys, or SMAs, use a phase change triggered by temperature change to change their shape and stiffness. Adaptive material actuators that modify the stiffness and shape of the structural element to which they are attached also function as an integral part of this structure because they also resist some of the internal loads.

Adaptive material actuators are used in roles where no efficient mechanical alternative exists. Vibration control using integrated active materials in a structure has been considered for orbiting space structures. As early as 1981, Swigert and Forward[3] suggested the use of piezoelectric transducers to damp bending vibration of a flexible mast.

Only recently have active adaptive materials been considered for atmospheric flight vehicle design. Proposed uses of adaptive materials for atmospheric flight vehicles have ranged from the control of a helicopter rotor blade using a piezoelectrically actuated trailing-edge flap[4,5] to use of piezoelectric materials for static aeroelastic control of a laminated composite wing.[6,7]

The earliest study of adaptive structure aerodynamic load generation is due to Crawley et al.[8] This study examined the use of piezoeletric actuators embedded in advanced composite plates to control lift on a surface with hypersonic flow over the upper and lower surfaces. Reference 9 expanded these studies to examine the response of piezoelectrically activated plates in an airstream. Chordwise curvature of the plate was used to generate aerodynamic loads, but no aeroelastic interaction was considered. Scott[10] examined the use of piezoelectric actuators for controlling the flutter of low-aspect ratio, high-speed wings. Reference 11 examined the use of piezoelectrics for dynamic control of a wing section.

The effectiveness of such schemes has been a subject of intense debate and research. Reference 7 discusses nondimensional parameters that can be used to evaluate effectiveness of active materials for changing wing lift effectiveness. A novel scheme for arranging piezoelectric elements to obtain twist and bending of beams was suggested by Lee.[12] Barrett has developed and demonstrated devices to control twist of helicopter blades.[5,13]

These flight vehicle structural control schemes generally use aeroelastic phenomena—created by mutual interaction between shape-dependent aerodynamic loads and structural deformation—to control the flight of the vehicle or to stabilize elements of the vehicle in flight. The control devices, e.g., ailerons, are called aeroservoelastic devices, and the control itself falls under the heading of aeroservoelasticity.

Aeroservoelasticity deals with the control of aeroelastic instabilities through the programmed use of integrated, controlled actuation forces, and moments. These control forces and moments are usually produced by moving aerodynamic surfaces such as ailerons. However, in the case discussed in this article, the aerodynamic forces are produced by imbedded adaptive material elements that move the entire aerodynamic surface.

Scope

This article is subdivided into four sections. The first describes adaptive materials and presents a brief background designed to acquaint the unfamiliar reader with basic concepts that must be integrated together to control the panel. The second section describes the structural model, together with the integrated active material actuators. The third section then focuses on the development of a method of control law development to link the actuators to the panel response. Finally, the results are discussed and parameters developed to help assess the effectiveness of different actuators for the control of panel flutter.

The origin of the panel flutter control problem will be discussed first. A Rayleigh-Ritz analytical model to analyze panel flutter with an adaptive material will be developed. The properties of the two adaptive materials 1) piezoelectrics and 2) shape memory alloys will be described to give the interested reader a background necessary to understand the issues of actuator integration. Finally, several examples will be considered to illustrate the use and effectiveness of these materials in integrated panel design.

Panel Flutter Control Microactuation

Innovative design uses for adaptive materials require curiosity about which phenomena lend themselves to effective control with this concept. Studies have indicated that replacement of existing aeroservoelastic devices with active, adaptive materials has limitations.[7,8] The use of large control surfaces to control aeroservoelastic response of large lifting surfaces may be categorized as macroactuation. Macroactuation requires large-scale changes in flow over a lifting surface. These large-scale changes are provided by aerodynamic surfaces that are usually preexisting for some other purpose. Questions about system complexity and cost effectiveness of adaptive material concepts have posed an obstacle to using adaptive structure concepts for macroactuation, because the materials must be added to an existing design.

On the other hand, adaptive material actuators also have been proposed for microactuation and microcontrol of aerodynamic phenomena. Microactuation uses small control devices to control flow over small critical parts of the structure. An example of passive microactuation might include a small vortex generator on a wing surface. Active microactuation concepts range from control of the pressure distribution on the upper surface of a transonic airfoil to reduce drag to the present study of controlling panel flutter on small portions of a flight structure.

Panel flutter is a much studied phenomenon that depends upon diverse factors such as local flow Mach number, flow angle with respect to the panel (sweep or yaw), edge support conditions, curvature, in-plane stress, and cavity effects.[13] It is primarily a supersonic flow phenomenon, although, in subsonic flow, it can take the form of static divergence or "aeroelastic buckling." Panel flutter is caused by the interaction between certain vibration modes created by the aerodynamic pressures on the panel as it oscillates. This aeroelastic interaction tends to draw certain natural frequencies of vibration together to coalesce. When this coalescence occurs, the panel becomes unstable.

In terms of the number of archival publications it has generated during the past four decades, panel flutter ranks among

the most interesting and the most studied of all aeroelastic phenomena. Reference 15 refers to panel flutter as a ". . . problem which has caused analytical difficulties out of all proportion to its apparent complexity. . . ." The surveys in Refs. 14 and 16 contain about 250 panel flutter publications; additional studies continue to appear to this day.

Reference 16 credits the first recognition of panel flutter to in-flight failures of 60–70 German V-2 rockets due to aeroelastic instabilities in the outer skin of this rocket. The first analytical study of panel flutter in 1949 was an investigation of the behavior of buckled panels exposed to supersonic flow. Shortly thereafter, in 1950, Miles[17] presented the first credible study of panel flutter as a dynamic phenomenon. The studies that appeared over the next 25 yr read like a Who's Who in aeroelasticity and unsteady aerodynamics.

Panel flutter has been well-researched, and analytical methods for its study are well-developed. These methods have ranged from simple linear models of so-called two-dimensional models with an infinite dimension in the crossflow direction, to more complicated models that include structural and flow nonlinearities.[18,19] Design criteria for panel design are also well-developed and are covered in Refs. 16 and 20.

The amplitude of panel flutter oscillation is limited by geometric nonlinearities, created by out-of-plane deformation, that augment plate bending stiffness resistance to out-of-plane motion.[21] As a result, when a panel flutters, the stresses are small enough so that limit cycle oscillations of the panel occur instead of the explosive failure associated with lifting surface flutter.

Because skin panels have low bending stiffness, there is a possibility that microactuators could be effective aeroservoelastic devices to control panel response. This idea was first examined by Scott.[10] A study of optimizing the panel weight by proper placement and controlled thickness of piezoelectric devices that changed panel in-plane stiffness was done later by Hajela and Glowasky.[22] One problem with this concept is that flutter speed can be raised by simply increasing the panel thickness. On the other hand, there may be other instances where actuator sensor combinations are attached to the panel for other reasons and can also be multifunctional and control flutter.

The rectangular panel used in this study is shown in Fig. 1. Supersonic flow over the upper surface is directed in the x direction. A thin piezoelectric actuator with electrodes attached top and bottom is shown in Fig. 2. Piezoelectric materials accumulate an electric charge proportional to a mechanical stress imposed on the material and, conversely, an electric field across the electrodes will cause the material to expand or contract.[23,24]

Applying a voltage across the electrodes in Fig. 2 creates an electric field E_3 perpendicular to the poling direction of the material across the thickness of the piezoelectric material.

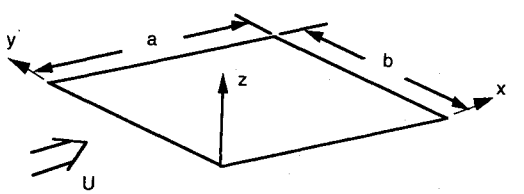

Fig. 1 Flat panel with flow and crossflow dimensions.

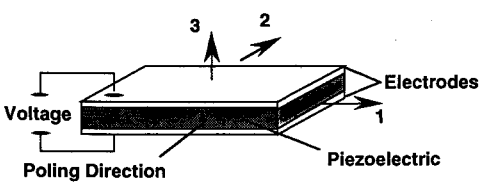

Fig. 2 Piezoelectric actuator.

The electric field is simply the voltage divided by the distance between the electrodes. This electric field causes the material to expand or contract, unless it is prevented from doing so by a neighboring material or restraint. There is a maximum allowable electric field that can be applied in the poling direction of piezoelectrics; fields of greater magnitude destroy the piezoelectric properties of the material. The electromechanical coupling constants and the depolarizing voltage (maximum voltage) are important material parameters for actuator design.

Piezoelectric materials can develop compressive or tensile strain, depending upon the polarity of the applied electric field or voltage. For relatively low electric field strength, the relationship between electric field and strain is linear. For larger fields, the relationship is nonlinear and the materials show significant hysteresis effects as the voltage across the material is cycled.[25]

The relationship between the stress and strain in directions 1 and 2 (x and y), shown in Fig. 2, and the transversely applied electric field, E_3, in direction 3 (z) reads

$$\begin{Bmatrix}\sigma_{11}\\ \sigma_{22}\\ \tau_{12}\end{Bmatrix} = \begin{bmatrix}Q_{11} & Q_{12} & 0\\ Q_{12} & Q_{22} & 0\\ 0 & 0 & Q_{66}\end{bmatrix}\left\{\begin{Bmatrix}\varepsilon_{11}\\ \varepsilon_{22}\\ \gamma_{12}\end{Bmatrix} - \begin{Bmatrix}d_{31}\\ d_{32}\\ 0\end{Bmatrix} E_3\right\} \tag{1}$$

The coefficients d_{ij} determine the material strain developed per unit of electric field applied across the actuator thickness. The coefficients Q_{ij} are orthotropic material stiffnesses. This relationship is similar to the relationship between stress, strain, and temperature change in a conventional orthotropic material.

When a piezoelectric layer of material is prevented from straining, the relationship between stress and piezoelectric strain is

$$\begin{Bmatrix}\sigma_{11}\\ \sigma_{22}\\ \tau_{12}\end{Bmatrix} = -\begin{bmatrix}Q_{11} & Q_{12} & 0\\ Q_{12} & Q_{22} & 0\\ 0 & 0 & Q_{66}\end{bmatrix}\begin{Bmatrix}d_{31}\\ d_{32}\\ 0\end{Bmatrix} E_3 \tag{2}$$

Note that, when the piezoceramic material is isotropic, the d_{31} and d_{32} terms are equal, and there is no coupling between normal stress and shear strain unless the material is applied in some special manner, such as suggested and demonstrated by Lee[12] or Barrett.[13] In addition, the combination of elastic moduli and piezoelectric constants d_{ij} determines the actuator strength, as indicated in Eq. (2). The larger the product $Q_{ij}d_{ij}$, the more effective will be the actuator.

Two piezoelectric actuator materials are considered in this study, lead zirconate titanate (PZT) and polyvinylidene fluoride (PVDF). PZT is a brittle piezoceramic material whose elastic modulus is close to aluminum. It has isotropic piezoelectric behavior. PVDF is a piezopolymer with a relatively low elastic modulus compared to aluminum. The ratio of d_{31} to d_{32} is about 10, so it can be reoriented to couple together normal stress and shear strain.[24] Strain actuators are most effective when their stiffness is nearly the same as the structure they are trying to control.[26] Since piezopolymers are inherently much less stiff than piezoceramics, and piezoceramics have stiffnesses similar in magnitude to conventional panel materials like aluminum, piezopolymers are generally less effective actuators for panel flutter applications.

A second type of microactuators for panel flutter are the so-called shape memory alloy materials, or SMAs. Shape memory alloy actuators have the ability to return to a "memorized" shape because of a phase change caused by heating the material. Nitinol®, developed in 1965,[27] is the most common shape memory material. Nitinol has two unique capabilities. First, plastic strains up to 8% can be fully recovered. This means that the material, when heated, can reduce its dimensions as much as 8%.

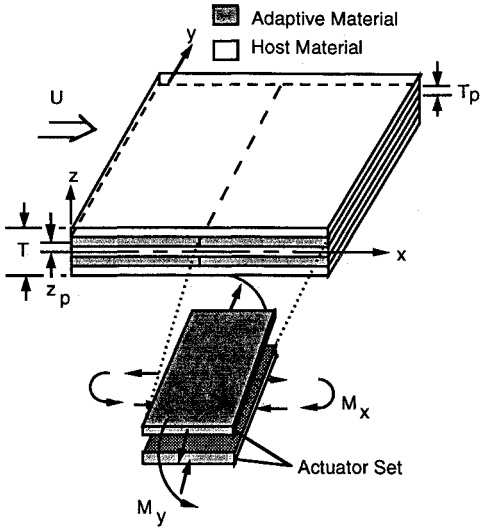

Fig. 3 Panel with adaptive actuators.

If the material is fixed at its boundaries and cannot expand or contract, then stresses are set up in the material equal to the strain recovery value times the Young's modulus of the material. Theoretically, stresses of up to 100,000 psi can be generated by constraining a shape memory alloy actuator from returning to its memorized shape.

When heated, the Young's modulus of Nitinol increases by a factor of 3–4. The temperature change required to cause the material to return to its memorized shape, and increase its elastic modulus, can be obtained by resistive heating of Nitinol fibers.[18] Supersonic panels have their own heat source provided by the flow.

As indicated in Fig. 3, piezoelectric materials and Nitinol can be embedded or surface-mounted. Advantages of embedding adaptive materials in the host structure include increasing the efficient load transfer from the actuator material to the host structure and reducing surface contamination of the structure with fragile components and connections. In atmospheric vehicle applications, embedded installation is required to protect the components from damage by the airflow and to avoid destroying the surface geometry characteristics that affect lift and drag.

While both piezoelectric and SMA actuators can be embedded in panels, they have very different capabilities. Piezoelectric materials respond quickly to an applied voltage, while SMAs like Nitinol require a longer time to respond, because temperature changes occur slowly. This means that piezoelectric materials have a large bandwidth, making them more suitable for feedback control schemes, while Nitinol is more appropriately used in on/off control situations.

Analytical Model

This study requires a model that can capture the essential features of the panel flutter control problem, but still generate results that can be understood. The flat panel model uses laminated plate theory to model the plate bending response to aerodynamic loads normal to the plate. The model has four essential elements: 1) the panel inertia, 2) the panel stiffness, 3) the panel airloads, and 4) the panel actuators. Each of these elements is represented by a matrix of elements.

The purpose of this section is to illustrate the development of these four arrays of elements and to document the equations of motion. The airloads are represented using linearized theory.[15] A Rayleigh-Ritz approach was adopted to solve the partial differential equations for the system eigenvalues. These eigenvalues contain the required stability information for the panel.

The equations of motion are represented in nondimensional matrix form, using modal coordinates and assuming simple harmonic motion at frequency ω, are as follows:

$$-\omega^2[\bar{M}_{ij}]\{\zeta_i\} + [\bar{K}_{ij} - \lambda\bar{B}_{ij}]\{\zeta_i\} = \{\bar{Q}_i\} \tag{3}$$

where ζ_i is the generalized coordinate for the ith mode, and $\{\bar{Q}_i\}$ represents the generalized forces due to the actuators. Part of the aerodynamic forces information is contained in $[\bar{B}_{ij}]$, while the effect of the airspeed and Mach number of the supersonic airstream is contained in the parameter λ. When the terms on the right side of Eq. (3) are zero and λ is also equal to zero, Eq. (3) provides the equations for a conservative system vibrating in a vacuum. In this case, the natural frequencies (eigenvalues) ω are real numbers.

Panel flutter is due primarily to a coalescence of two natural vibration modes created by aerodynamic coupling. When λ is not zero, the equations of motion are non-self-adjoint and the "frequencies" may be either real or complex conjugate, depending upon the value of λ. This parameter may be increased from zero until two of the frequencies coalesce or become identical. This value of the pressure parameter that creates coalescence is the critical value of λ for the panel. Above λ_{cr}, these two frequencies will be complex conjugates of each other. Because of the assumption of simple harmonic motion, this signals panel dynamic instability.

Which two panel modes coalesce, and how many modes are required to obtain an acceptable solution for flutter, depend on the panel length to width ratio, a/b, and the bending stiffness of the panel. Reference 18 suggests at least four normal modes of vibration as appropriate for defining flutter accurately. On the other hand, for orthotropic panels, or for panels with large values of a/b, more modes are necessary to create an accurate solution. Reference 28 indicates that for panels where $0 < a/b < 1$, four modes are sufficient for predicting λ_{cr}.

When the actuator terms on the right side of Eq. (3) are functions of the displacement, they will affect the eigenvalue problem and will either stabilize or destabilize the panel. To solve the controlled panel problem, let us first develop the expressions for the mass and stiffness matrices in Eq. (3).

Referring to Fig. 1, the out-of-plane deformation w is assumed to be given by the following series expression:

$$w(x, y, t) = \sum_{i=1}^{N} \psi_i(x, y)\zeta_i(t) \tag{4}$$

The functions ψ_i represent the spatial distributions of orthogonal vibration mode shapes when the panel is vibrating in a vacuum. These modes are given by

$$\psi_i(x, y) = \sin(m_i\pi x/a)\sin(n_i\pi y/b) \tag{5}$$

Because we will use full-state feedback to generate actuator feedback control laws, a premium is placed upon the size of the analytical model. Our panel model retains the first four vibration modes of the plate ($m_i = 1, 2, 3, 4$ and $n_i = 1, 1, 1, 1$). While more modes could be included in the computation, convergence studies with our model and our aspect ratios indicated that these four were sufficient to illustrate the effects we intended.

Elements of the mass $[M]$ and stiffness $[K]$ matrices are obtained by applying Lagrange's equations to expressions for the plate kinetic energy and the plate strain energy, respectively. The general expressions for the elements of these matrices are

$$M_{ij} = \int_0^b \int_0^a m_0\psi_i\psi_j \, dx \, dy \tag{6}$$

$$k_{ij} = \iint \left(D_{11} \frac{\partial^2 \Psi_i}{\partial x^2} \frac{\partial^2 \Psi_j}{\partial x^2} + D_{22} \frac{\partial^2 \Psi_i}{\partial y^2} \frac{\partial^2 \Psi_j}{\partial y^2} + 2D_{12} \frac{\partial^2 \Psi_i}{\partial x^2} \frac{\partial^2 \Psi_j}{\partial y^2} + 4D_{66} \frac{\partial^2 \Psi_i}{\partial x \partial y} \frac{\partial^2 \Psi_j}{\partial x \partial y} \right) dx\, dy - \iint_A \left(N_x \frac{\partial^2 \Psi_j}{\partial x^2} + N_y \frac{\partial^2 \Psi_j}{\partial y^2} + 2N_{xy} \frac{\partial^2 \Psi_j}{\partial x \partial y} \right) \Psi_i \, dx\, dy \tag{7}$$

where m_0 is the plate mass per unit area (this mass changes when actuators are substituted for primary plate structure), D_{11}, D_{22}, D_{12}, and D_{66} are the integrated plate and actuator bending stiffnesses, and N_x, N_y, and N_{xy}, are in-plane forces per unit length (positive for compression).[29] The in-plane loads are assumed constant and are not functions of panel displacement.

For an isotropic material, $D_{11} = D_{22} = ET^3/[12(1 - \nu^2)]$, $D_{12} = \nu D_{11}$, and $D_{66} = GT^3/12$, where E, G, and ν are the material properties of the plate material, and T is the thickness of the plate. Note that the plate mass per unit area and the plate stiffness will depend on the cross-sectional arrangement of the plate, in particular the thickness and arrangement of actuator and plate structure material in the plate cross section.

Integrating Eqs. (6) and (7) and dividing the results by $D_{11}b/a^2$, nondimensional equations for the mass and stiffness elements become

$$\begin{aligned} \bar{M}_{ij} &= m_0 \frac{a^4}{4D_{11}} \qquad i = j \\ \bar{M}_{ij} &= 0 \qquad\qquad\quad i \neq j \end{aligned} \tag{8}$$

$$\begin{aligned} \bar{K}_{ij} &= \pi^4 \left[m_i^4 + \frac{D_{22}}{D_{11}} \left(\frac{a}{b}\right)^4 n_i^4 + \left(2\frac{D_{12}}{D_{11}} + 4\frac{D_{66}}{D_{11}} \right) \left(\frac{a}{b}\right)^2 m_i^2 n_i^2 \right] + \frac{\pi^4}{4} \left[\frac{R_{xx}}{\pi^2} m_i^2 + \frac{R_{yy}}{\pi^2} \left(\frac{a}{b}\right)^2 n_i^2 \right] \qquad i = j \\ \bar{K}_{ij} &= 0 \qquad\qquad\qquad\qquad\qquad\qquad\qquad\qquad\qquad\qquad\qquad\qquad\qquad\qquad\qquad\qquad\qquad\quad i \neq j \end{aligned} \tag{9}$$

where R_{xx} and R_{yy} are nondimensional in-plane loads in the x and y directions, respectively.

To include the effects of air moving supersonically over one side of the panel, piston theory is used to calculate the pressure loading on the panel Δp. This expression for the pressure is[15]

$$\Delta p = \frac{\rho U^2}{\sqrt{M^2 - 1}} \left(\frac{\partial w}{\partial x} + \frac{1}{U} \frac{M^2 - 2}{M^2 - 1} \frac{\partial w}{\partial t} \right) \tag{10}$$

The $\partial w/\partial t$ term in Eq. (10) provides a relatively small damping effect on panel flutter speed and is not included in this analysis.[15]

The matrix $[\bar{B}_{ij}]$ in Eq. (1) relates the aerodynamic forces to the panel generalized displacements. Using the relation in Eq. (10), we define elements

$$B_{ij} = \frac{\rho U^2}{\sqrt{M^2 - 1}} \int_0^b \int_0^a \frac{\partial \Psi_j}{\partial x} \Psi_i \, dx\, dy \tag{11}$$

and divide the elements by $D_{11}b/a^2$ and λ to obtain

$$\begin{aligned} \bar{B}_{ij} &= \frac{m_i}{4} \left\{ \frac{1}{m_i - m_j} + \frac{1}{m_i + m_j} - \frac{\cos[\pi(m_i - m_j)]}{m_i - m_j} - \frac{\cos[\pi(m_i + m_j)]}{m_i + m_j} \right\} \qquad i \neq j \\ \bar{B}_{ij} &= 0 \qquad\qquad\qquad\qquad\qquad\qquad\qquad\qquad\qquad\qquad\qquad\qquad\qquad\qquad\qquad\qquad\qquad\quad i = j \end{aligned} \tag{12}$$

The adaptive material actuators are arranged in a sandwich configuration in the upper and lower halves of the panel, as shown in Fig. 3. To cause bending of the plate, the upper and lower actuators are stimulated simultaneously by voltages with opposite signs. Laminated plate theory is used to compute the moments generated by embedded active actuator layers in the plate.[29]

The actuator layers are segmented in the y direction. The theory used here does not account for any decreased stiffness because of this discontinuity between actuator segments. It assumes that a perfect bond exists between segments.

The plate resultant normal forces and moments are related to the plate midplane strains ε and plate curvatures κ by

$$\begin{Bmatrix} \boldsymbol{N} \\ \boldsymbol{M} \end{Bmatrix} = \begin{bmatrix} A & B \\ B & D \end{bmatrix} \begin{Bmatrix} \varepsilon^0 \\ \kappa \end{Bmatrix} - \begin{Bmatrix} \boldsymbol{N}_\Lambda \\ \boldsymbol{M}_\Lambda \end{Bmatrix} \tag{13}$$

where $\{\boldsymbol{N}\}$ and $\{\boldsymbol{M}\}$ are vectors of forces and moments per unit length, respectively.[30] The A, B, and D matrices are those defined in laminated composite theory. Note that the $[B_{ij}]$ matrix in Eq. (13) has a different meaning than it does in Eq. (12).

The terms $\boldsymbol{N}_\Lambda$ and $\boldsymbol{M}_\Lambda$ in Eq. (13) represent the actuator forces and moments, respectively. $\boldsymbol{N}_\Lambda$ and $\boldsymbol{M}_\Lambda$ are written as

$$\{\boldsymbol{N}_\Lambda\} = \sum_{k=1}^{2} [T_\varepsilon]_k^T [Q_{ij}]_k \{\Lambda\}_k t_k \tag{14}$$

$$\{\boldsymbol{M}_\Lambda\} = \sum_{k=1}^{2} [T_\varepsilon]_k^T [Q_{ij}]_k \{\Lambda\}_k z_k t_k \tag{15}$$

Here, t_k is the thickness of the kth actuator layer, while z_k is the distance from the midplane to the centroid of the kth actuator layer. For piezoelectric materials $\Lambda_1 = E_3 d_{31}$ and $\Lambda_2 = E_3 d_{32}$, while for SMA actuators, Λ_1 and Λ_2 represent the recovery strain. In this case these magnitudes are less than 0.08. Equations (14) and (15) also include the matrix of actuator elastic constants $[Q_{ij}]$ and the transformation matrix of direction cosines $[T_\varepsilon]$ to transform $[Q_{ij}]$ to the global coordinate system. In this study the actuator material is assumed isotropic so that $[T_\varepsilon]$ is an identity matrix.

To control panel flutter with active bending moments, the ith nondimensional generalized force is found by using Eq. (15) and the mode shapes to create the following expression:

$$\bar{Q}_i = \frac{a^2}{D_{11}b} \int_0^b \int_0^a \begin{Bmatrix} -\dfrac{\partial^2 \Psi_i}{\partial x^2} \\ -\dfrac{\partial^2 \Psi_i}{\partial y^2} \\ -2\dfrac{\partial^2 \Psi_i}{\partial x \partial y} \end{Bmatrix} \{\boldsymbol{M}_\Lambda\} \, dx\, dy \tag{16}$$

Substituting for the elastic constants in Eq. (15), we have

$$\{M_\Lambda\} = 2T_pZ_p \begin{bmatrix} \frac{E_p}{1-v^2} & \frac{vE_p}{1-v^2} & 0 \\ \frac{vE_p}{1-v^2} & \frac{E_p}{1-v^2} & 0 \\ 0 & 0 & G_p \end{bmatrix} \begin{Bmatrix} d_{31} \\ d_{32} \\ 0 \end{Bmatrix} E_3 \quad (17)$$

The applied voltage $V = E_3^* t_k$ is an actively controlled input to the panel actuators.

Static in-plane tensile forces increase the panel out-of-plane stiffness to increase flutter speed. Either piezoelectrics[22] or SMAs may be used to produce in-plane forces, written as

$$\{N_\Lambda\} = 2T_p \begin{bmatrix} \frac{E_p}{1-v^2} & \frac{vE_p}{1-v^2} & 0 \\ \frac{vE_p}{1-v^2} & \frac{E_p}{1-v^2} & 0 \\ 0 & 0 & G_p \end{bmatrix} \begin{Bmatrix} \Lambda_1 \\ \Lambda_2 \\ 0 \end{Bmatrix} \quad (18)$$

Actuator Generalized Forces

Using Eqs. (16) and (17), the expression for the ith generalized force due to the actuators is

$$Q_i = \left[\frac{2a \frac{E_p}{1-v^2} E_3^* d_{31} T_p Z_p}{D_{11}} \right] \times \sum_{s=1}^{NC} u_s \begin{bmatrix} 2\frac{m_i}{n_i} \cos\left(\frac{m_i p x}{a}\right)_{x_{s-1}}^{x_s} \\ 2\frac{n_i}{m_i}\left(\frac{a}{b}\right)^2 \cos\left(\frac{m_i p x}{a}\right)_{x_{s-1}}^{x_s} \\ 0 \end{bmatrix}^T \begin{Bmatrix} 1 + v\frac{d_{32}}{d_{31}} \\ v + \frac{d_{32}}{d_{31}} \\ 0 \end{Bmatrix} \quad (19)$$

In Eq. (19) the control input E_3 has been replaced by u_s; u_s is the fraction of the maximum allowable field E_3^* applied to the sth actuator set. An absolute value of u_s greater than unity means that the input field will depolarize the piezoelectric materials. NC is the number of actuator sets (in this case two), while x_s and x_{s-1} define the location of the edges of the sth actuator set. Equation (19) can be written as

$$\{\bar{Q}\} = P[g]\{u\} \quad (20)$$

where

$$P = \frac{\frac{E_p}{E_s} E_{3\max} d_{31} \frac{T_p}{T} \frac{Z_p}{T}}{\frac{T}{a}\frac{1}{3}\left\{1\left[\left(\frac{1}{2}\right)^3 - \left(\frac{Z_p}{T} + \frac{T_p}{2T}\right)^3 + \left(\frac{Z_p}{T} - \frac{T_p}{2T}\right)^3\right] + \frac{E_p}{E_s}\left[\left(\frac{Z_p}{T} + \frac{T_p}{2T}\right)^3 - \left(\frac{Z_p}{T} - \frac{T_p}{2T}\right)^3\right]\right\}} \quad (21)$$

Here, $[g]$ is a $N \times NC$ matrix (in this case, a 4×2), while $\{u\}$ is the $NC \times 1$ (in this case, a 2×1) vector of control inputs. E_p and E_s are the Young's moduli for the adaptive material and the host panel material, respectively.

P measures the strength or capability of the piezoelectric actuator. This parameter depends on actuator layer placement with respect to the midplane (Z_p/T), actuator to host material modulus ratio (E_p/E_s), electromechanical properties (the maximum value of the applied field E_3^* and d_{31}), and integrated plate stiffness and host material stiffness properties (D_{11}/E_p).

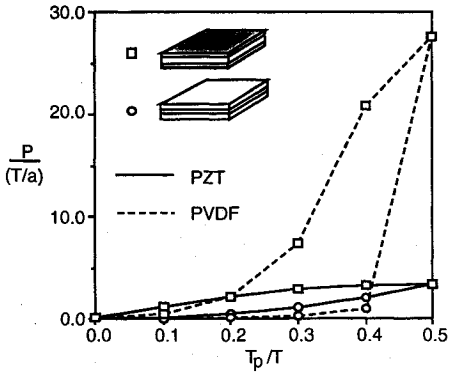

Fig. 4 Values of P [Eq. (21)] for an aluminum panel with two different actuator locations.

Note that the ratio (T_p/T) refers to the thickness of *one* of the actuator layers divided by the total panel thickness. As a result, the maximum value of this parameter is 0.5 when the panel is constructed solely of an adaptive material.

Values of P for the two extreme actuator locations (at the midplane and at the outer surfaces) are shown for PZT and PVDF in Fig. 4. The host material is aluminum, so that $E_p/E_s = 0.9$ for PZT and $E_p/E_s = 0.028$ for PVDF. P is proportional to the moment arm of the actuators with respect to the midplane of the panel, and inversely proportional to the bending stiffness of the panel. Thus, when a low modulus material like PVDF is used, a large value of P can be obtained because of the reduction in panel bending stiffness caused by replacing part of the host material with low modulus actuator materials.

Control Law Formulation

Control laws to drive the panel actuators are obtained by solving a linear quadratic regulator (LQR) problem for the gain matrix that stabilizes the system at a given design airspeed or Mach number. In this case, the parameter λ is fixed to a specified design value. The equations of motion, written in state-space form are

$$\{\dot{x}\} = [F]\{x\} + [G]\{u\} \quad (22)$$

where $[F]$, $[G]$, and $\{x\}$ are defined as

$$[F] = \begin{bmatrix} [0] & [I] \\ -[[\bar{M}]^{-1}[\bar{K} - \lambda\bar{B}]] & 0 \end{bmatrix} \quad (23)$$

$$[G] = \begin{bmatrix} [0] \\ P[\bar{M}]^{-1}[g] \end{bmatrix} \quad (24)$$

$$\{x\} = \begin{Bmatrix} \{\zeta\} \\ \{\dot{\zeta}\} \end{Bmatrix} \quad (25)$$

The eigenvalues of $[F]$ determine whether or not the open-loop system is stable or unstable. The critical value of non-dimensional dynamic pressure parameter, above which the open loop panel is unstable, is referred to as λ_{cr}.

The full-state feedback control problem is defined when the control input vector $\{u\}$ is equal to the product of a feedback gain matrix $[k]$ and the state vector $\{x\}$:

$$\{u\} = -[k]\{x\} \tag{26}$$

The gain matrix $[k]$ in Eq. (26) is obtained by solving the continuous-time LQR problem and the associated algebraic Riccati equations. If a solution to this problem exists, stability of the panel is guaranteed. The LQR feedback gain matrix $[k]$ is one that minimizes the cost function

$$J = \int_0^\infty (\{x\}^T[Q]\{x\} + \{u\}^T[R]\{u\})\, dt \tag{27}$$

subject to the constraint of Eq. (23), where $[Q]$ and $[R]$ are weighting matrices. Note that the $[Q]$ matrix in Eq. (27) has an entirely different meaning than when used for the laminate elastic moduli matrix in previous equations. When $[Q]$ is set to [0] the minimum control solution is obtained. If more than one actuator is used, the values of $[R]$ are selected to force all actuators to be used at their fullest capacity.

Control law development requires a design airspeed and altitude condition. This means that λ must be specified in Eq. (23). For a given panel geometry and value of P, the open-loop (control off) nondimensional flutter dynamic pressure λ_{cr} is used as a starting point. The value of λ is then increased slightly, and the LQR control law represented by $[k]$ is obtained to stabilize the system. The system response is checked to see if the actuator voltages are within bounds. The value of λ can be increased until, at some special value of λ, the actuators cannot stabilize the panel without becoming saturated. The value of λ for which the elements of $\{u\}$ reach a magnitude of unity and become ineffective is defined as λ_{sat}.

Two points about this model should be emphasized before continuing. The control law design approach requires a system perturbation or disturbance. The saturation level of the actuators depends on the size of this perturbation. In practice, the perturbation would be provided by the turbulent boundary layer next to the panel. Model complexity is minimized if an initial panel deflection is used as a perturbation instead of a more complicated disturbance. The perturbation used to excite the panel is an initial deflection of the panel in the first mode so that ζ_1/a is between 0.005–0.010.

The second point is that, while nondimensionalization is a useful tool to identify parameter combinations, it can cause misinterpretations of analytical results if not examined properly. To illustrate this potential difficulty, Fig. 5 presents the results of an analysis displayed two ways: 1) nondimensionally, and 2) in terms of airspeed at constant Mach number. The upper half of Fig. 5 compares nondimensional flutter dynamic pressure (λ_{cr}) and control saturation dynamic pressure (λ_{sat}) of two different panels. One panel has piezoelectric layers ($T_p/T > 0$), while the other ($T_p/T = 0$) has none. The flutter airspeeds for the two panels are shown in the lower half of Fig. 5.

The panels considered for this study hold the cross-sectional thickness fixed so that we substitute actuator material for panel host material. Until the panel becomes active, such a substitution may reduce, not increase, the open-loop flutter speed. To understand this, notice that in Fig. 5 two conditions apply to a panel with piezoelectric actuators: 1) the open-loop (OL) case with no control activation, and 2) the closed-loop (CL) case with active piezoelectric actuators.

The parameter λ_{cr}, by definition, is the same for both the open-loop piezoelectric panel and the nonpiezoelectric panel. On the other hand, the flutter dynamic pressures and airspeeds of the two panels are different because they have different cross sections and different bending stiffnesses. Increases in flutter velocity (at a constant Mach number) occur only when the product λD_{11} is increased, since dynamic pressure is proportional to the product of panel bending stiffness D_{11} and the nondimensional dynamic pressure λ.

Because E_p of most piezoelectrics is less than typical panel materials such as aluminum, the OL flutter airspeed of a panel constructed with piezoelectrics is less than that of a nonpiezoelectric panel, even when the parameter λ_{cr} is the same for both. In Fig. 5, active control is effective until λ_{sat}. The gray area shown in Fig. 5 represents the range of values where the actuator(s) become saturated. The actuator saturation velocity U_{sat} may be less than (lower part of gray area) or greater (upper part of gray area) than U_{cr} of the nonadaptive panel without piezoelectric elements. Therefore, if the saturation velocity of the actuators is not above the dashed line in Fig. 5 then, with panel thickness constrained, the use of piezoelectric actuators for controlling panel flutter cannot be justified.

Discussion of Results

The results of active and passive panel flutter control methods are presented in this section. The panel host material is aluminum, and the analysis is restricted to the case of d_{32}/d_{31}, equal to unity. The number of actuator segments and their division points (x_s and x_{s+1}) depends on the shape of the vibration mode to be controlled. An actuator is most effective for control of a particular mode if the sign of the strain due to the modal deflection shape is the same over the entire actuator.

Figure 6 shows the flutter mode displacement and surface strain profile for an infinite aspect-ratio panel (a/b approaching zero). The flutter mode resembles a combination of the first and second free vibration modes of the panel. This mode has a change in curvature at $x/a = 0.58$, so that the piezoelectric actuator is divided into two parts at that point.

Figure 7 plots actuator saturation dynamic pressure parameter values against values of P when either one or two actuator sets are used. LQR methods are used to design control laws. As seen in Fig. 7, for a given value of P, the value

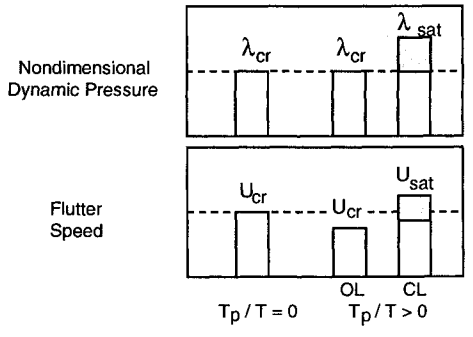

Fig. 5 Effects on panel stability of replacing panel material with actuator material.

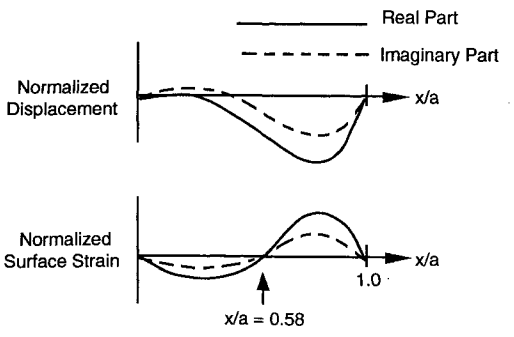

Fig. 6 Flutter mode and corresponding surface strain distribution, $a/b = 0$.

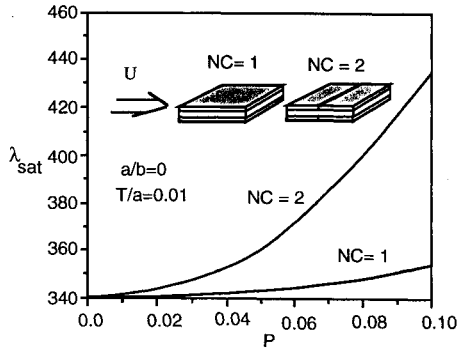

Fig. 7 λ_{sat} vs P.

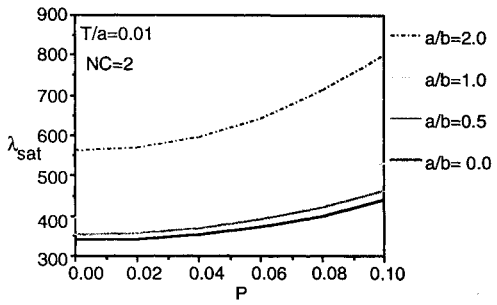

Fig. 8 λ_{sat} vs P for four different aspect ratios with initial panel deflection of $0.01a$.

of λ_{sat} is much larger when the actuation layers are divided into two sets. While the first mode is equally controllable with either one or two actuator sets, the second mode is far more controllable with two actuators. The control of the second mode is a requirement for controlling flutter. As a result, the rest of the discussion is confined only to panels where the actuator set is divided into two actuators at $x/a = 0.58$.

The effect of panel aspect ratio b/a on the ability to control flutter is shown in Fig. 8. Here, λ_{sat} is plotted against P with four different panel aspect ratios. When panel aspect ratio is reduced (a/b increased), the percentage improvement in the flutter value of λ from λ_{cr} to λ_{sat} is increased. Equation (19) shows that smaller aspect ratios (larger a/b terms) lead to larger piezoelectric generalized forces. On the other hand, the aerodynamic stiffness terms in Eq. (12) are not increased for smaller aspect ratios. Therefore, the actuators are relatively more effective for panels having smaller aspect ratios.

Figures 9 and 10 plot the normalized flutter airspeed vs thickness ratio for two panel thicknesses, assuming that all other parameters are held constant. Figure 9 ($T/a = 0.01$) shows that the only case where the flutter speed is increased is where PZT is used with the smaller initial deflection. Even then, this increase is very small.

For a thinner panel ($T/a = 0.005$), Fig. 10 indicates that the flutter airspeed increases when PZT actuators are used, particularly when a small initial disturbance is used. These figures demonstrate that integrating the piezoelectric materials into the panel, i.e., reducing the amount of host material, while adding actuators, particularly PVDF, will reduce the open-loop flutter airspeed. In this study, only PZT showed potential for increasing panel flutter airspeed once the loop is closed. The detrimental effects of PVDFs low modulus far outweigh any "increases" made in the flutter velocity from its open-loop condition.

The parameter P appears to be a good indicator of an actuator's ability to increase the closed-loop flutter airspeed above the open-loop flutter velocity. On the other hand, a large value of this parameter is no guarantee to improved performance, because it may correspond to situations where the open-loop flutter velocity is reduced significantly due to the removal of panel material and replacement by piezoelectric material.

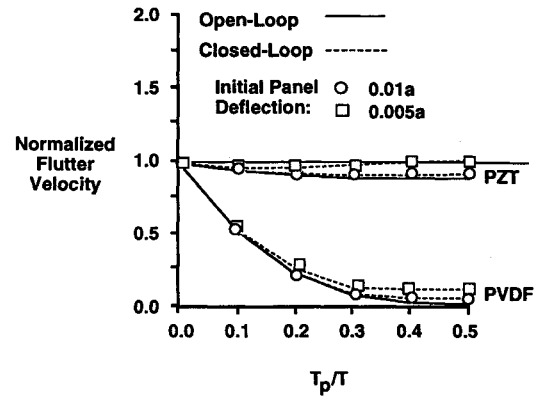

Fig. 9 Normalized flutter velocities vs thickness ratio, $T/a = 0.01$ and $a/b = 0$.

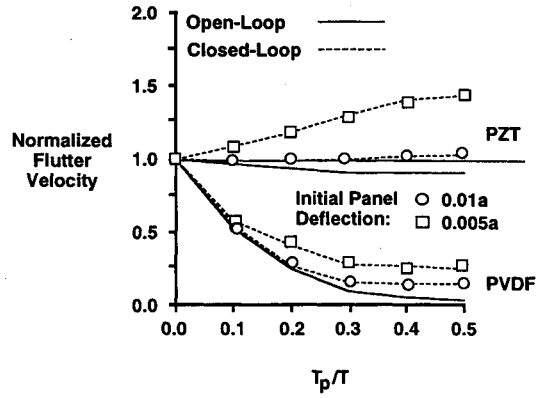

Fig. 10 Normalized flutter velocities vs thickness ratio, $T/a = 0.005$ and $a/b = 0$.

Control of Panel In-Plane Forces

The panel flutter speed can be increased by using adaptive materials to create in-plane tensile forces. These in-plane forces change the in vacuo panel natural frequency spacing and increase the flutter speed. With passive in-plane stiffness control, only an on/off command is required, and there is no need for a complicated control law.

When using piezoelectrics materials to create in-plane forces, an applied voltage creates the same actuation strain on both upper and lower actuators. No net moments are created. Both the nondimensional in-plane forces and the panel stiffness matrix are changed, as shown in Eq. (9). The placement of the adaptive layers with respect to the panel midplane has no effect on the size of the in-plane forces. Therefore, the actuator layers are placed at the midplane of the panel so that changes in panel bending stiffness due to the adaptive materials are reduced. Using Eq. (14), the nondimensional in-plane force in the flow direction due to piezoelectric materials is calculated to be

$$R_{xx} = \frac{2(E_p/E_s)E_3^* d_{31}(T_p/T)[1 + \nu(d_{32}/d_{31})]}{(T/a)^2(D_{11}/E_s T^3)} \tag{28}$$

The expression for R_{yy} is similar. The nondimensional inplane force for a shape memory alloy actuator is

$$R_{xx} = \frac{2(E_p/E_s)(T_p/T)\Lambda_x}{(T/a)^2(D_{11}/E_s T^3)} \tag{29}$$

where Λ_x is the free strain that the SMA can recover when heated.

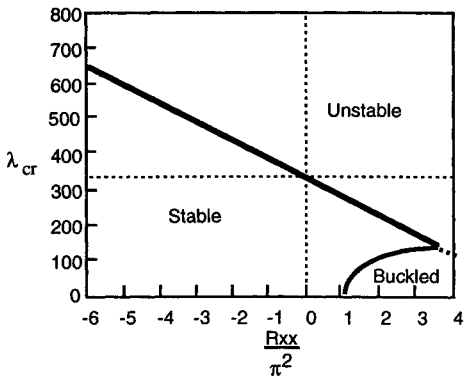

Fig. 11 λ_{cr} **vs in-plane load,** $a/b = 0$.

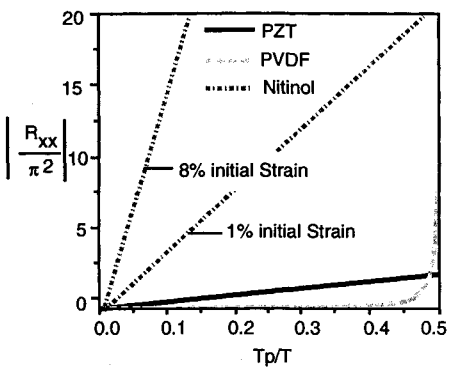

Fig. 12 Nondimensional in-plane load vs thickness ratio, $T/a = 0.01$.

The general effect of panel inplane loads on λ_{cr} is shown in Fig. 11. Positive values of R_{xx} (compressive loading) cause a reduction in λ_{cr}, and eventually cause the panel to buckle if they are too high. Negative values of R_{xx} (tensile loading) created by adaptive materials will cause λ_{cr} to increase. Absolute values of R_{xx}/π^2 vs thickness ratio for three panels with $T/a = 0.01$, and each constructed with a different adaptive material, are shown in Fig. 12. These results assume that the maximum electric field is applied to the piezoelectric materials. Initial strains of 1 and 8% are assumed for Nitinol. A stiffness increase of 200% is also included when modeling Nitinol in its "actuated" state. Figure 12 shows that Nitinol can provide much more in-plane force than piezoelectric materials.

Recent studies by Weisshaar and Sadlowski[31] have used a NASTRAN finite element analysis to model thin panels with small shape memory actuators bonded to the lower surface. These actuators cover only a small portion of the panel surface. Their results show that the panel flutter speed can be increased substantially. In addition, the studies of Hajela and Glowasky[22] with piezoelectric actuators to increase in-plane forces support the conclusions of the present study.

Concluding Remarks

The use of adaptive material microactuation to control panel flutter has been suggested as a possible use of smart materials. Linear analytical panel models examined two flutter control methods; one method used dynamic active control while the other uses passive control with shape memory actuators. The piezoelectric actuators use full state feedback control laws obtained by solving a linear quadratic regulator problem. Panel thickness is held constant.

For panels where the first and second in vacuo modes are the primary contributor to the flutter mode, a minimum of two actuators are required to obtain significant increases in flutter speed over the open-loop condition. Piezoelectric materials have lower elastic moduli compared to the panel materials (aluminum or composites) that they replace. This results in a reduction in the open-loop flutter speed when piezoelectric materials are substituted for the original panel material. Active control increases the panel flutter speed, but it may not increase it above the original uncontrolled speed. As a result, it may be better to increase the panel flutter speed by simply adding more structural material.

It is important to note that in this study of actively controlling panel flutter, the controller saturation point was directly related to the perturbation used to excite the panel. The larger the perturbation, the lower the controller saturation velocity. The perturbation used in this system provided a means of determining how best to apply piezoelectric to the control of panel flutter. It did not, however, provide a definitive answer to the question of whether piezoelectrics should be used to control flutter at all. Future research utilizing high-fidelity analytical models using a turbulence model to excite the panel will provide this answer.

For the passive control method, piezoelectric materials and shape memory alloys were used to create in-plane forces to increase the panel out-of-plane stiffness. These in-plane forces increase and separate the frequencies of the in vacuo vibration modes, thereby delaying the modal coupling and increasing the flutter speed. The analysis showed that the shape memory alloy Nitinol can induce much larger in-plane forces than can the piezoelectrics. The stimulus for activating Nitinol is heat. Since aerodynamic heating creates compressive stresses that reduce panel flutter speed, Nitinol may provide a very simple and effective means of controlling of flutter in heated panels.

References

[1]Weisshaar, T. A., "Aeroelastic Tailoring, Creative Uses of Unusual Materials," *Proceedings of the 28th Structures, Structural Dynamics and Materials Conference*, Monterey, CA, April 1987 (AIAA Paper 87-0976).

[2]Wada, B. K., Fanson, J. L., and Crawley, E. F., "Adaptive Structures," *Proceedings of the ASME Winter Annual Meeting*, Dallas, TX, Dec. 1990.

[3]Swigert, C. J., and Forward, R. L., "Electronic Damping of Orthogonal Bending Modes in a Cylindrical Mast—Theory," *Journal of Spacecraft and Rockets*, Vol. 18, No. 1, 1980, pp. 5–10.

[4]Spangler, R. L., Jr., "Piezoelectric Actuators for Helicopter Rotor Control," M.S. Thesis, Massachusetts Inst. of Technology, Cambridge, MA, 1989.

[5]Barrett, R. M., "Intelligent Rotor Blade Actuation Through Directionally Attached Piezoelectric Crystals," 46th American Helicopter Society Forum, Washington, DC, 1990.

[6]Ehlers, S. M., and Weisshaar, T. A., "Static Aeroelastic Behavior of an Adaptive Laminated Piezoelectric Composite Wing," *Proceedings of the 31st SDM Conference*, Long Beach, CA, April 1990, pp. 1611–1623.

[7]Weisshaar, T. A., and Ehlers, S. M., "Adaptive Aeroelastic Composite Wings—Control and Optimization Issues," *Composites Engineering*, Vol. 2, Nos. 5–7, 1992, pp. 457–476.

[8]Crawley, E. F., Warkintin, D. J., and Lazarus, K. B., "Feasibility Analysis of Piezoelectric Devices," Massachusetts Inst. of Technology Systems Lab., Aeronautics and Astronautics Dept., Rept. SSL 5-88, Cambridge, MA, Jan. 1988.

[9]Lazarus, K. B., Crawley, E. F., and Bohlmann, J. D., "Static Aeroelastic Control Using Strain Actuated Adaptive Structures," *Proceedings of the U.S.-Japan Conference on Adaptive Materials and Structures*, Maui, HI, Nov. 1990, pp. 197–223.

[10]Scott, R. C., "Control of Flutter Using Adaptive Materials," M.S. Thesis, School of Aeronautics and Astronautics, Purdue Univ., West Lafayette, IN, May 1990.

[11]Lazarus, K. B., Crawley, E. F., and Lin, C. Y., "Fundamental Mechanisms of Aeroelastic Control with Control Surface and Strain Actuation," *Proceedings of the 32nd SDM Conference*, Baltimore, MD, April 1991, pp. 1817–1831.

[12]Lee, C.-K., "Piezoelectric Laminates for Torsional and Bending Modal Control: Theory and Experiment," Ph.D. Dissertation, Cornell Univ., Ithaca, NY, 1987.

[13]Barrett, R. M., "Method and Apparatus for Structural Actuation and Sensing in a Desired Direction," U.S. Patent Application 485,599, Feb. 1990.

[14]Dowell, E. H., "NASA Space Vehicle Design Criteria, Panel Flutter," NASA SP-8004, July 1964 (Revised 1972).

[15]Ashley, H., and Zartarian, G., "Piston Theory—A New Aerodynamic Tool for the Aeroelastician," *Journal of the Aeronautical Sciences*, Vol. 23, No. 12, 1956, pp. 1109–1118.

[16]Lemley, C. E., "Design Criteria for the Prediction and Prevention of Panel Flutter, Volume I: Criteria Presentation, Volume II: Background and Review of the State-of-the-Art," Air Force Flight Dynamics Lab. TR-67-140, Wright-Patterson AFB, OH, Dec. 1967.

[17]Miles, J. W., "Dynamic Chordwise Stability at Supersonic Speeds," North American Aviation Inc., Rept. AL-1140, Los Angeles, CA, Oct. 1950.

[18]Dowell, E. H., *Aeroelasticity of Plates and Shells*, Noordhoff International Publishing, Leyden, The Netherlands, 1975.

[19]Librescu, L., *Elastostatics and Kinetics of Anisotropic and Heterogeneous Shell-Type Structures*, Noordhoff International Publishing, Lyden, 1975.

[20]Laurenson, R. L., and McPherson, J. I., "Design Procedures for Flutter-Free Surface Panels," NASA CR-2801, March 1977.

[21]Dowell, E. H., "Nonlinear Oscillations of a Fluttering Plate," *AIAA Journal*, Vol. 4, No. 7, 1966, pp. 1267–1275.

[22]Hajela, P., and Glowasky, R., "Application of Piezoelectric Elements in Supersonic Panel Flutter Suppression," AIAA/AHS/ASEE Aircraft Design Systems and Operations Meeting, AIAA Paper 91-3191, Baltimore, MD, Sept. 1991.

[23]Jaffe, B., Cook, W. R., and Jaffe, H., *Piezoelectric Ceramics*, Academic Press, London and New York, 1971.

[24]Parton, V. Z., and Kudryaztsev, B. A., *Electromagnetoelasticity*, Gordon and Breach, New York, 1988.

[25]Bryant, M. D., and Keltie, R. F., "A Characterization of the Linear and Non-Linear Dynamic Performance of a Practical Piezoelectric Actuator Part 1: Measurements," *Sensors and Actuators*, Vol. 9, 1986, pp. 95–103.

[26]Crawley, E. F., and de Luis, J., "Use of Piezoelectric Actuators as Elements of Intelligent Structures," *AIAA Journal*, Vol. 25, No. 10, 1987, pp. 1373–1385.

[27]Buehler, W. J., and Wiley, R. C., "Nickel-Based Alloys," U.S. Patent 3,174,851, March 23, 1965.

[28]Bisplinghoff, R. L., and Ashley, H., *Principles of Aeroelasticity*, Wiley, New York, 1962, pp. 403–437.

[29]Jones, R. M., "Mechanics of Composite Materials," Scripta, Washington, DC, 1975.

[30]Crawley, E. F., and Lazarus, K. B., "Induced Strain Actuation of Isotropic and Anisotropic Plates," *Proceedings of the 30th Structures, Structural Dynamics and Materials Conference*, Mobile, AL, 1989, pp. 1451–1461 (AIAA Paper 89-1326).

[31]Weisshaar, T. A., and Sadlowski, M. J., "The Effects of SMA Micro-Actuation on Panel Flutter," School of Aeronautics and Astronautics, Purdue Univ., AAE Rept. 92-100, West Lafayette, IN, Aug. 1992.